Electronic Supplementary Information
for

Solvent and Electrolyte Effects on $Ni(P^{R}_{2}N^{R'}_{2})_{2}$-Catalyzed Electrochemical Oxidation of Hydrogen

*Ryan M. Stolley, Jonathan M. Darmon, and Monte L. Helm**
Correspondence to monte.helm@pnnl.gov

PDF file includes:

Table of Contents
Materials and Methods

Table of Contents

Materials and Methods S3

Materials S3

Instrumentation S3

Figure S1. Cyclic volatammograms of fluorobenzene and THF solutions of $Ni(P^{Cy}_2N^{Bn}_2)_2$ as a function of supporting electrolyte. S4

Figure S2. Cyclic volatammograms of fluorobenzene and THF solutions of $Ni(P^{Cy}_2N^{tBu}_2)_2$ as a function of supporting electrolyte. S5

Figure S3. Plot of the peak current (i_p) versus (scan rate)$^{1/2}$ for $Ni(P^{Cy}_2N^{Bn}_2)_2$ in fluorobenzene. . S6

Figure S4. Plot of the peak current (i_p) versus (scan rate)$^{1/2}$ for $Ni(P^{Cy}_2N^{Bn}_2)_2$ in THF. . . S7

Figure S5. Plot of the peak current (i_p) versus (scan rate)$^{1/2}$ for $Ni(P^{Cy}_2N^{Bn}_2)_2$ in PhCN. . . S8

Figure S6. Plot of the peak current (i_p) versus (scan rate)$^{1/2}$ for $Ni(P^{Cy}_2N^{tBu}_2)_2$ in fluorobenzene. . S9

Figure S7. Plot of the peak current (i_p) versus (scan rate)$^{1/2}$ for $Ni(P^{Cy}_2N^{tBu}_2)_2$ in THF. . . S10

Figure S8. Identification of variables needed to calculate k_{obs}. S11

Figure S9. Cyclic volatammograms of $Ni(P^{Cy}_2N^{Bn}_2)_2$ in fluorobenzene upon addition of ^{n}BuNH$_2$.. S12

Figure S10. Cyclic volatammograms of $Ni(P^{Cy}_2N^{Bn}_2)_2$ in THF upon addition of ^{n}BuNH$_2$. . . S13

Figure S11. Cyclic volatammograms of $Ni(P^{Cy}_2N^{Bn}_2)_2$ in PhCN upon addition of ^{n}BuNH$_2$. . S14

Figure S12. Cyclic volatammograms of $Ni(P^{Cy}_2N^{Bn}_2)_2$ as a function of scan rate in THF with ^{n}BuNH$_2$. S15

Figure S13. Cyclic volatammograms of $Ni(P^{Cy}_2N^{tBu}_2)_2$ in fluorobenzene upon addition of ^{n}BuNH$_2$. S16

Figure S14. Cyclic volatammograms of $Ni(P^{Cy}_2N^{tBu}_2)_2$ in THF upon addition of ^{n}BuNH$_2$. . . S17

Figure S15. Plot of the catalytic current (i_{cat}) versus the concentration of ^{n}BuNH$_2$ for $Ni(P^{Cy}_2N^{Bn}_2)_2$. S18

Figure S16. Plot of the catalytic current (i_{cat}) versus the concentration of ^{n}BuNH$_2$ for $Ni(P^{Cy}_2N^{tBu}_2)_2$. S19

References S20

Materials and Methods

Materials

All manipulations were carried out using standard vacuum line, Schlenk and inert atmosphere glovebox techniques. Solvents were purified by passage through neutral alumina using an Innovative Technology, Inc., PureSolv™ solvent purification system. Water was dispensed from a Millipore MilliQ purifier (ρ = 18.2 MΩ·cm) and was degassed using three freeze-pump-thaw cycles prior to use. All amines used for electrocatalysis were dried over KOH or CaH_2, degassed, distilled under vacuum, and stored in a nitrogen-filled glovebox. Both $Ni(P^{Cy}_2N^{Bn}_2)_2$ (1) and $Ni(P^{Cy}_2N^{tBu}_2)_2$ (2) were prepared using literature procedures.

Instrumentation

All electrochemical procedures were conducted at ambient temperature, 23 ºC, under dinitrogen using either standard Schlenk conditions or a Vacuum Atmospheres drybox. A standard three-electrode configuration was employed in conjunction with a CH Instruments potentiostat interfaced to a computer with CH Instruments 700 D software. All voltammetric scans were recorded using glassy-carbon working electrode disks of 1 mm diameter (Cypress Systems EE040). A glassy-carbon rod (Structure Probe, Inc.) was used as the auxiliary electrode. A platinum wire (Alfa-Aesar) suspended in a solution of the electrolyte and separated from the analyte solution by a Vycor frit (CH Instruments 112) served as a pseudo-reference electrode. All glassware for electrochemical experiments was oven dried overnight and allowed to cool to room temperature before use. $[Cp^*_2Co][PF_6]$ and $[Cp_2Co][PF_6]$ were used as an internal standard, and all potentials reported within this work are referenced to the ferrocenium/ferrocene couple at 0.00 V. Bases were measured and transferred to electrochemical solutions via gas-tight syringes.

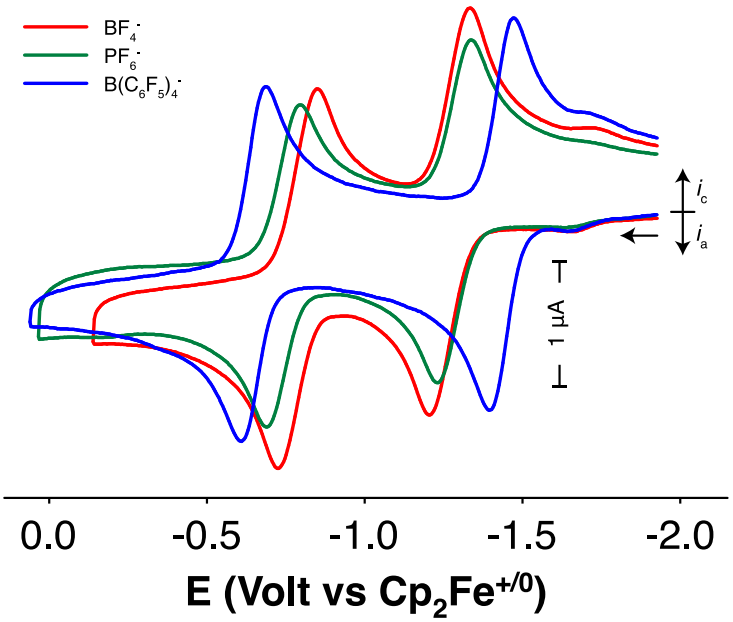

(a)

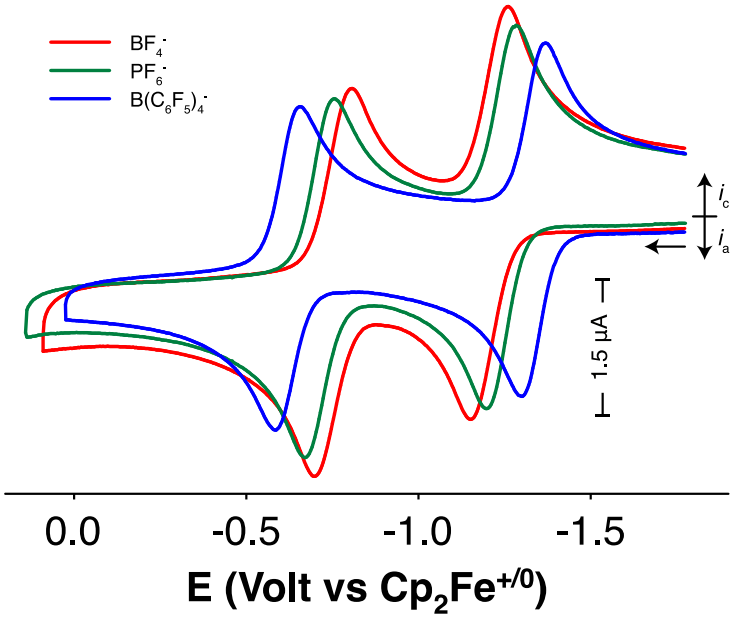

(b)

Figure S1. Cyclic volatommograms of a (a) fluorobenzene and (b) THF solution of $Ni(P^{Cy}_2N^{Bn}_2)_2$ utilizing [^{n}Bu$_4$N][BF$_4$] (red), [^{n}Bu$_4$N][PF$_6$] (green), and [^{n}Bu$_4$N][B(C$_6$F$_5$)$_4$] (blue) as the supporting electrolyte. Conditions: 0.8 mM [Ni], 0.2 M electrolyte, **scan rate**. Potentials are referenced to $Cp_2Fe^{+/0}$.

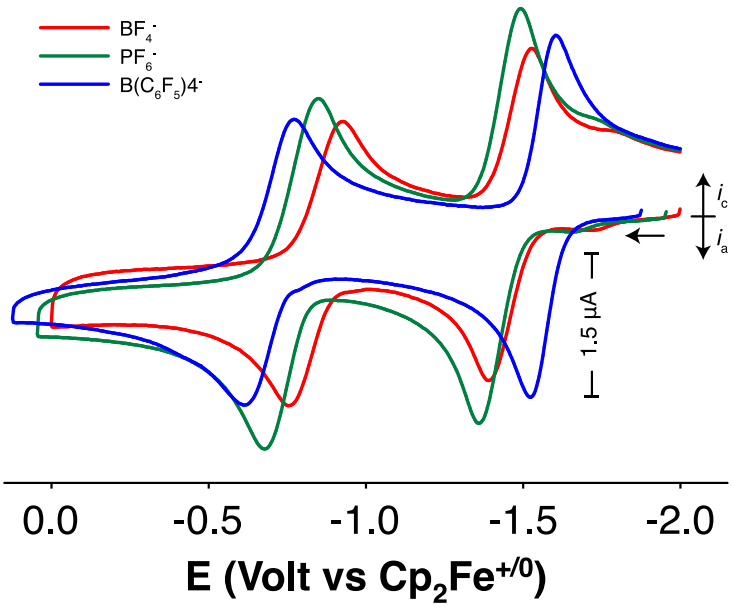

(a)

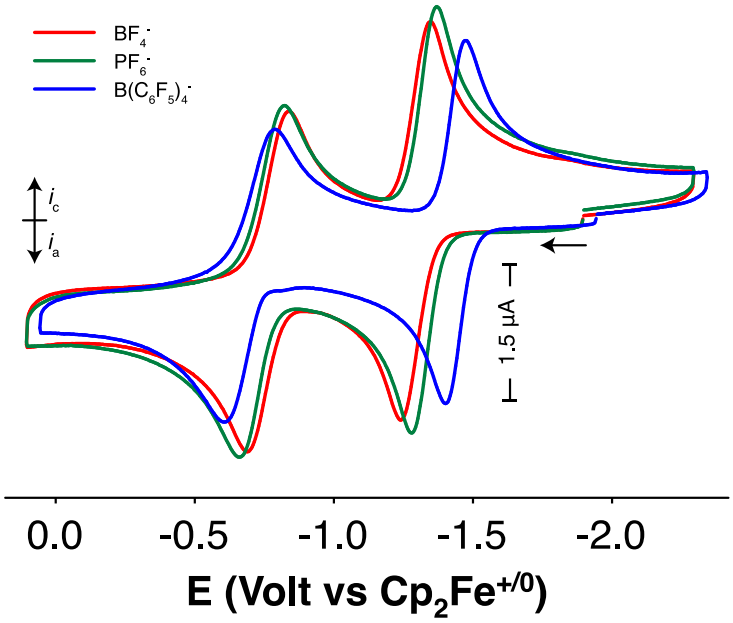

(b)

Figure S2. Cyclic volatammograms of a (a) fluorobenzene and (b) THF solution of $Ni(P^{Cy}_2N^{tBu}_2)_2$ utilizing $[^nBu_4N][BF_4]$ (red), $[^nBu_4N][PF_6]$ (green), and $[^nBu_4N][B(C_6F_5)_4]$ (blue) as the supporting electrolyte. Conditions: 0.8 mM [Ni], 0.2 M electrolyte, **scan rate**. Potentials are referenced to $Cp_2Fe^{+/0}$.

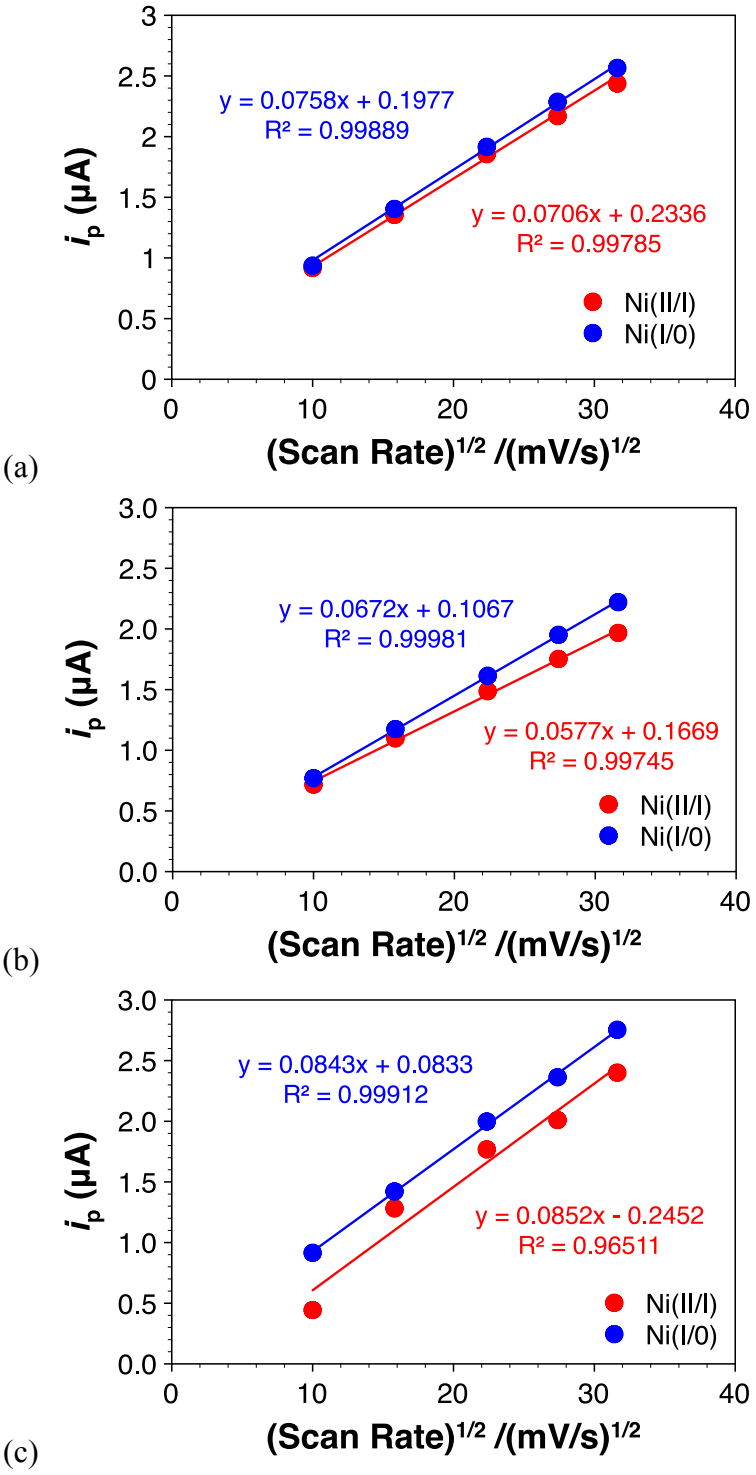

Figure S3. Plot of the peak current (i_p) for the Ni(II/I) and Ni(I/0) redox couples of Ni($P^{Cy}_2N^{Bn}_2$)$_2$ versus the square root of the scan rate in fluorobenzene solution using (a) [^{n}Bu$_4$N][BF$_4$], (b) [^{n}Bu$_4$N][PF$_6$], and (c) [^{n}Bu$_4$N][B(C$_6$F$_5$)$_4$] as the supporting electrolyte. Conditions: 0.8 mM [Ni], 0.2 M electrolyte.

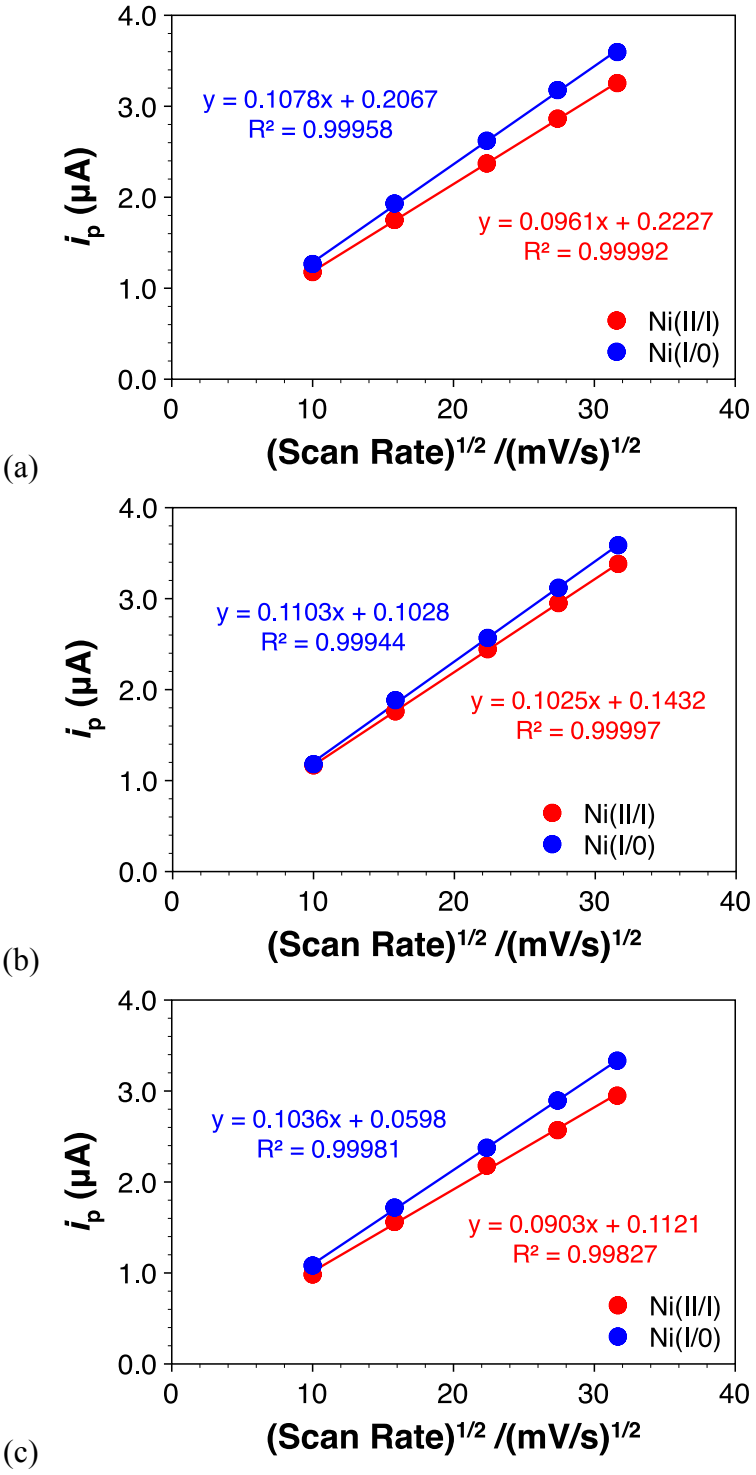

Figure S4. Plot of the peak current (i_p) for the Ni(II/I) and Ni(I/0) redox couples of Ni($P^{Cy}_2N^{Bn}_2$)$_2$ versus the square root of the scan rate in THF solution using (a) [^{n}Bu$_4$N][BF$_4$], (b) [^{n}Bu$_4$N][PF$_6$], and (c) [^{n}Bu$_4$N][B(C$_6$F$_5$)$_4$] as the supporting electrolyte. Conditions: 0.8 mM [Ni], 0.2 M electrolyte.

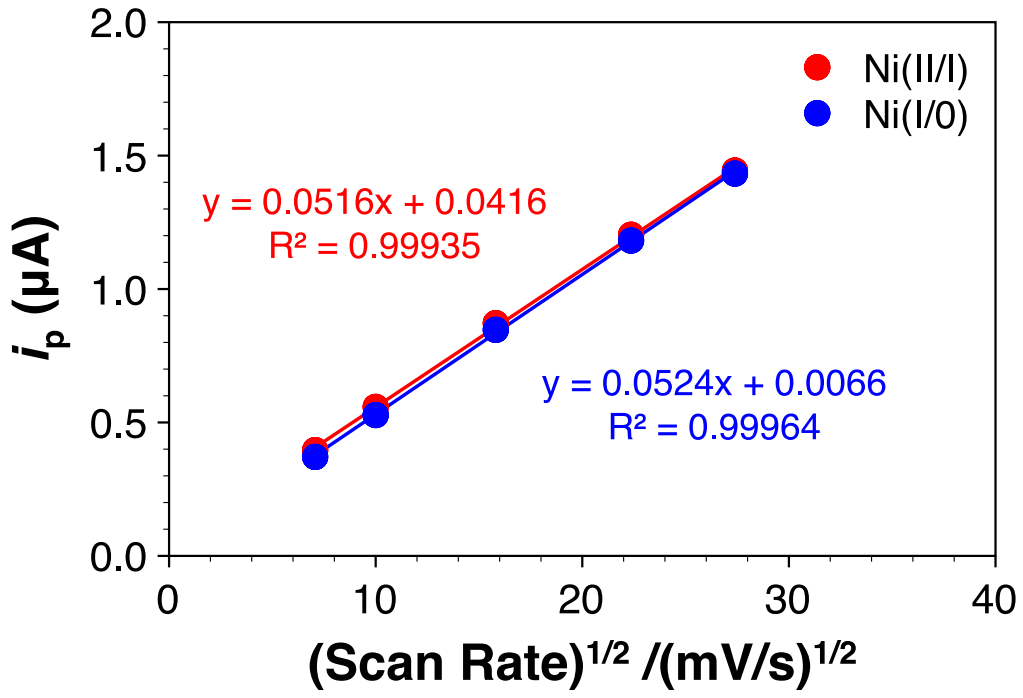

Figure S5. Plot of the peak current (i_p) for the Ni(II/I) and Ni(I/0) redox couples of Ni($P^{Cy}_2N^{Bn}_2$)$_2$ versus the square root of the scan rate in benzonitrile solution using [^{n}Bu$_4$N][PF$_6$] as the supporting electrolyte. Conditions: 0.8 mM [Ni], 0.2 M electrolyte.

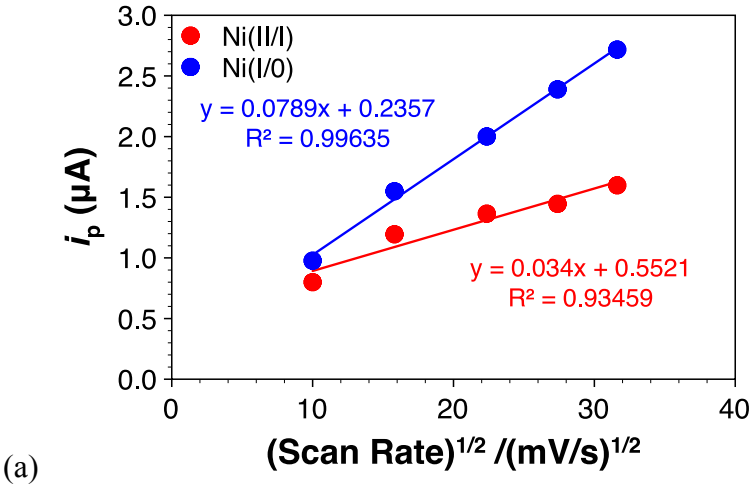

(a)

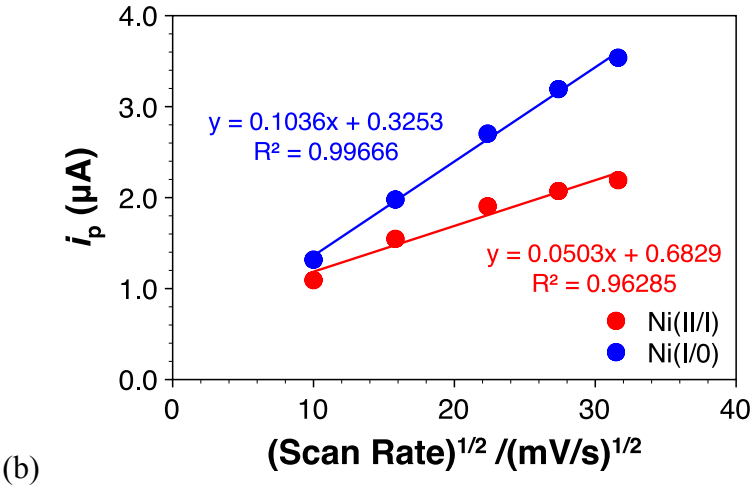

(b)

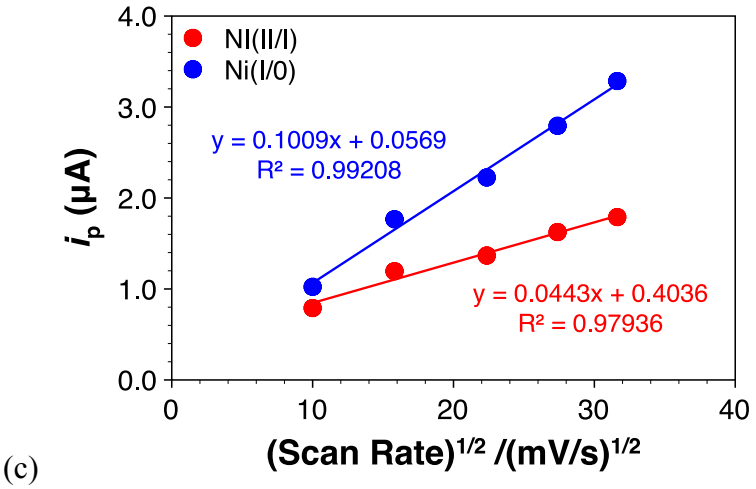

(c)

Figure S6. Plot of the peak current (i_p) for the Ni(II/I) and Ni(I/0) redox couples of Ni($P^{Cy}_2N^{tBu}_2$)$_2$ versus the square root of the scan rate in fluorobenzene solution using (a) [^{n}Bu$_4$N][BF$_4$], (b) [^{n}Bu$_4$N][PF$_6$], and (c) [^{n}Bu$_4$N][B(C$_6$F$_5$)$_4$] as the supporting electrolyte. Conditions: 0.8 mM [Ni], 0.2 M electrolyte.

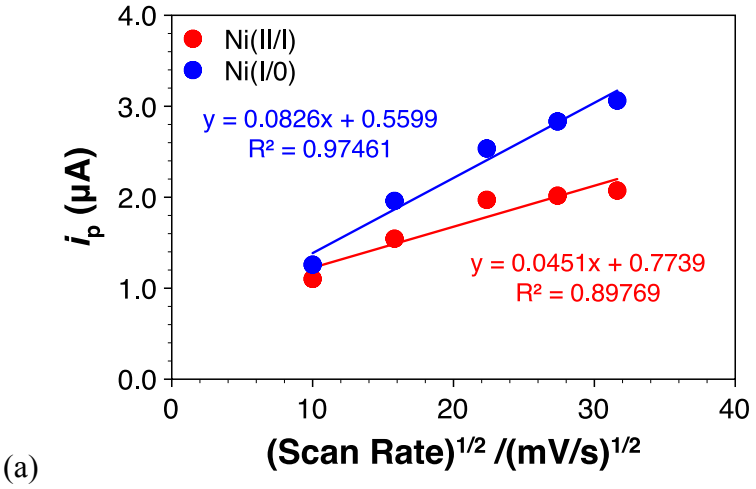

(a)

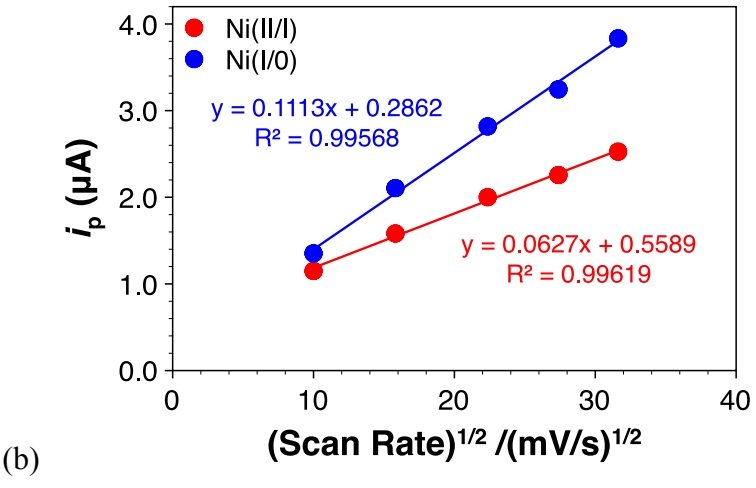

(b)

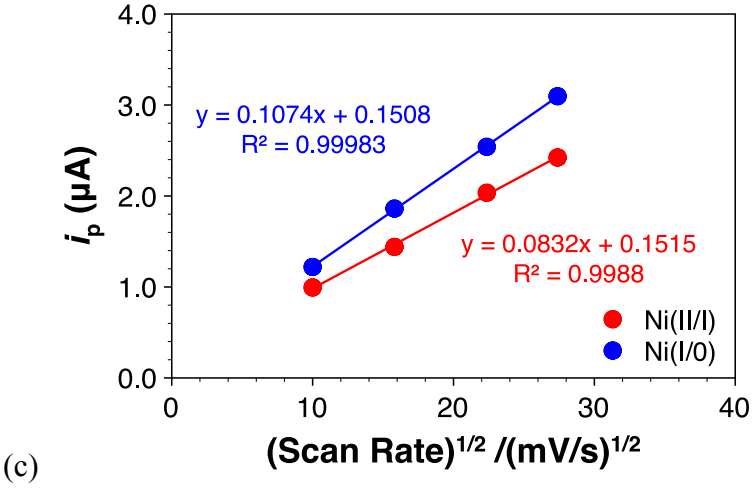

(c)

Figure S7. Plot of the peak current (i_p) for the Ni(II/I) and Ni(I/0) redox couples of Ni($P^{Cy}_2N^{tBu}_2$)$_2$ versus the square root of the scan rate in THF solution using (a) [^{n}Bu$_4$N][BF$_4$], (b) [^{n}Bu$_4$N][PF$_6$], and (c) [^{n}Bu$_4$N][B(C$_6$F$_5$)$_4$] as the supporting electrolyte. Conditions: 0.8 mM [Ni], 0.2 M electrolyte.

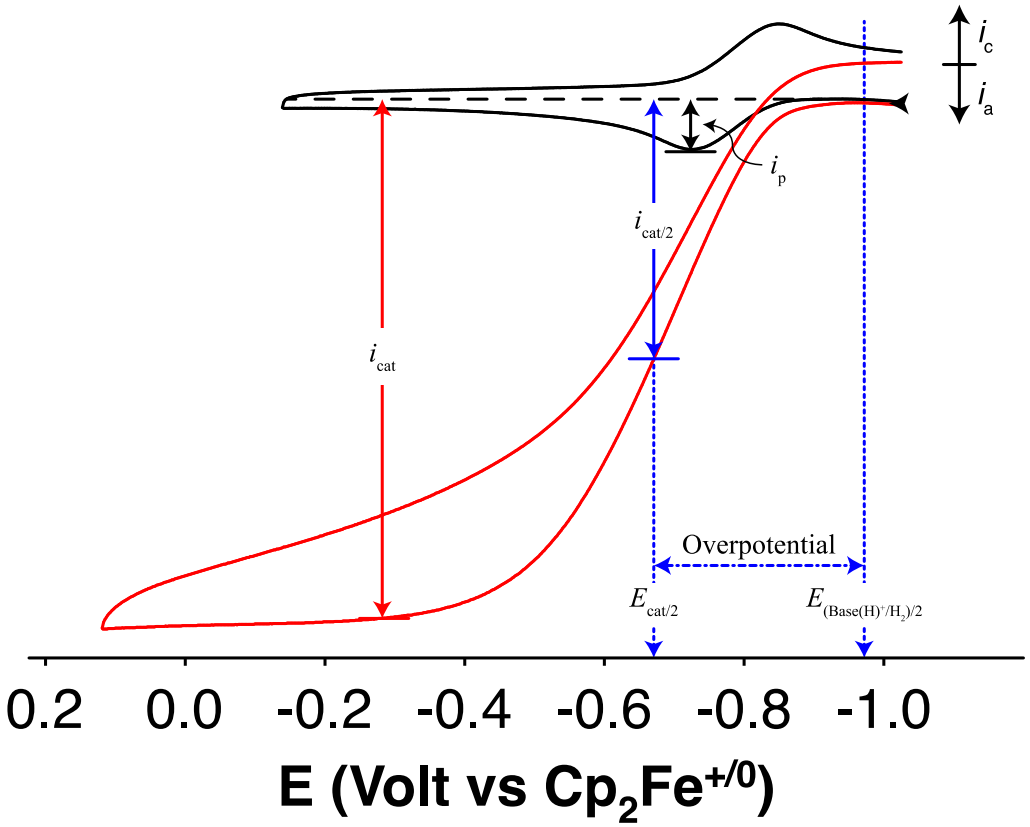

Figure S8. Cyclic voltammograms of a fluorobenzene solution of $Ni(P^{Cy}_2N^{Bn}_2)_2$ (*black*) and subsequent current enhancement upon addition of 55 mM ^{n}BuNH$_2$ (*red*).

Determination of turnover frequency (k_{obs}):

Turnover frequencies (k_{obs}) were determined from the ratio of i_{cat}/i_p using eq. 1, where n is the number of electrons (2 for H_2 oxidation), R is the gas constant (8.314 J K^{-1} mol^{-1}), F is Faraday's constant (9.65 × 10^4 C/mol), T is the temperature (298 K), and υ is the scan rate in V/s. The equation was simplified for hydrogen oxidation in eq. 2.

$$k_{obs} = \left(\frac{0.4463}{n}\right)^2 \cdot \left(\frac{F\nu}{RT}\right) \cdot \left(\frac{i_{cat}}{i_p}\right)^2 \qquad \text{(eq. 1)}$$

$$k_{obs} = 1.94\, V^{-1} \cdot \nu \cdot \left(\frac{i_{cat}}{i_p}\right)^2 \qquad \text{(eq. 2)}$$

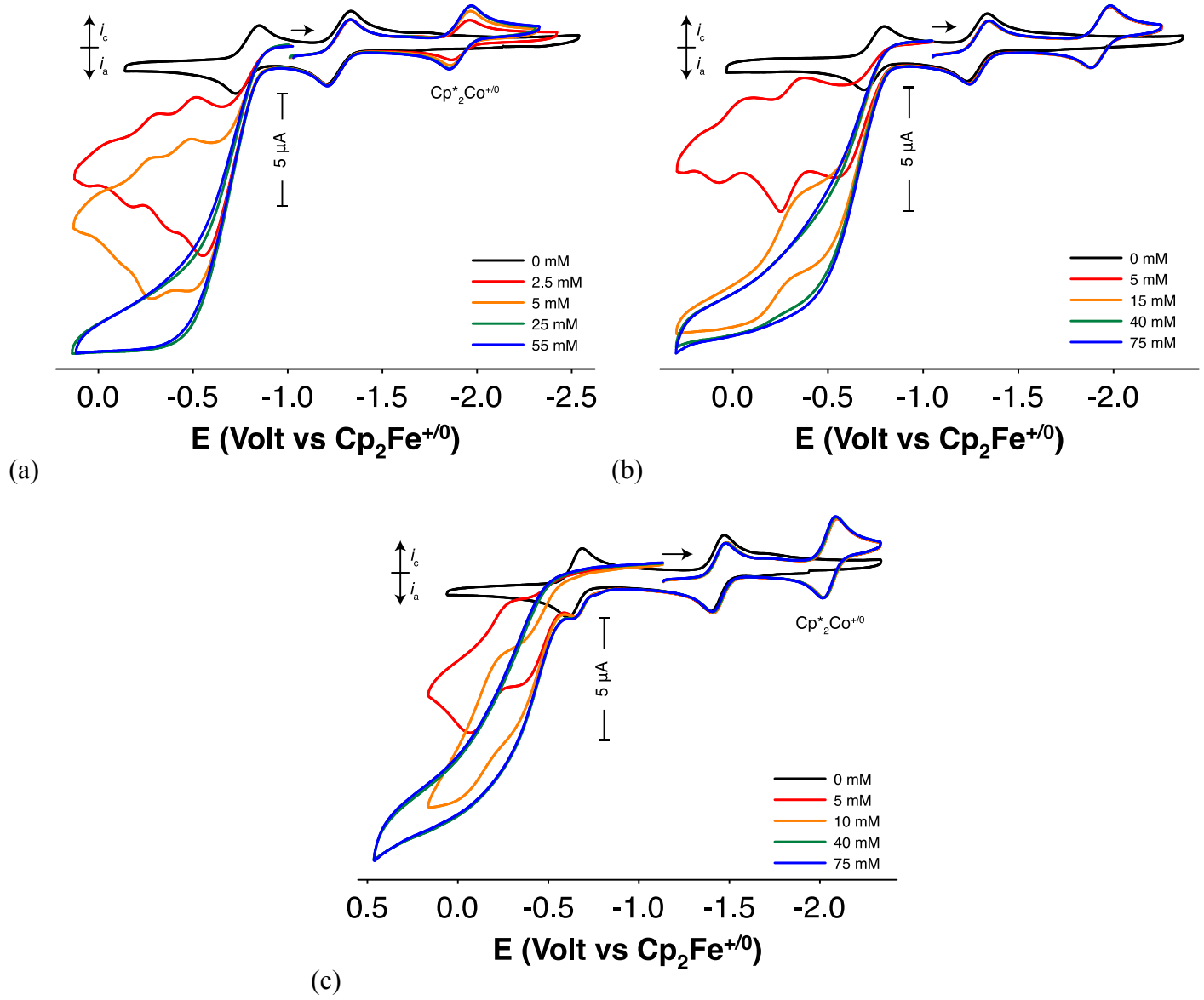

Figure S9. Cyclic volatommograms of a fluorobenzene solution of $Ni(P^{Cy}_2N^{Bn}_2)_2$ upon addition of ^{n}BuNH$_2$ using (a) [^{n}Bu$_4$N][BF$_4$], (b) [^{n}Bu$_4$N][PF$_6$], and (c) [^{n}Bu$_4$N][B(C$_6$F$_5$)$_4$] as the supporting electrolyte. Conditions: 0.8 mM [Ni], 0.2 M electrolyte, 250 mV/s. Potentials are referenced to $Cp_2Fe^{+/0}$.

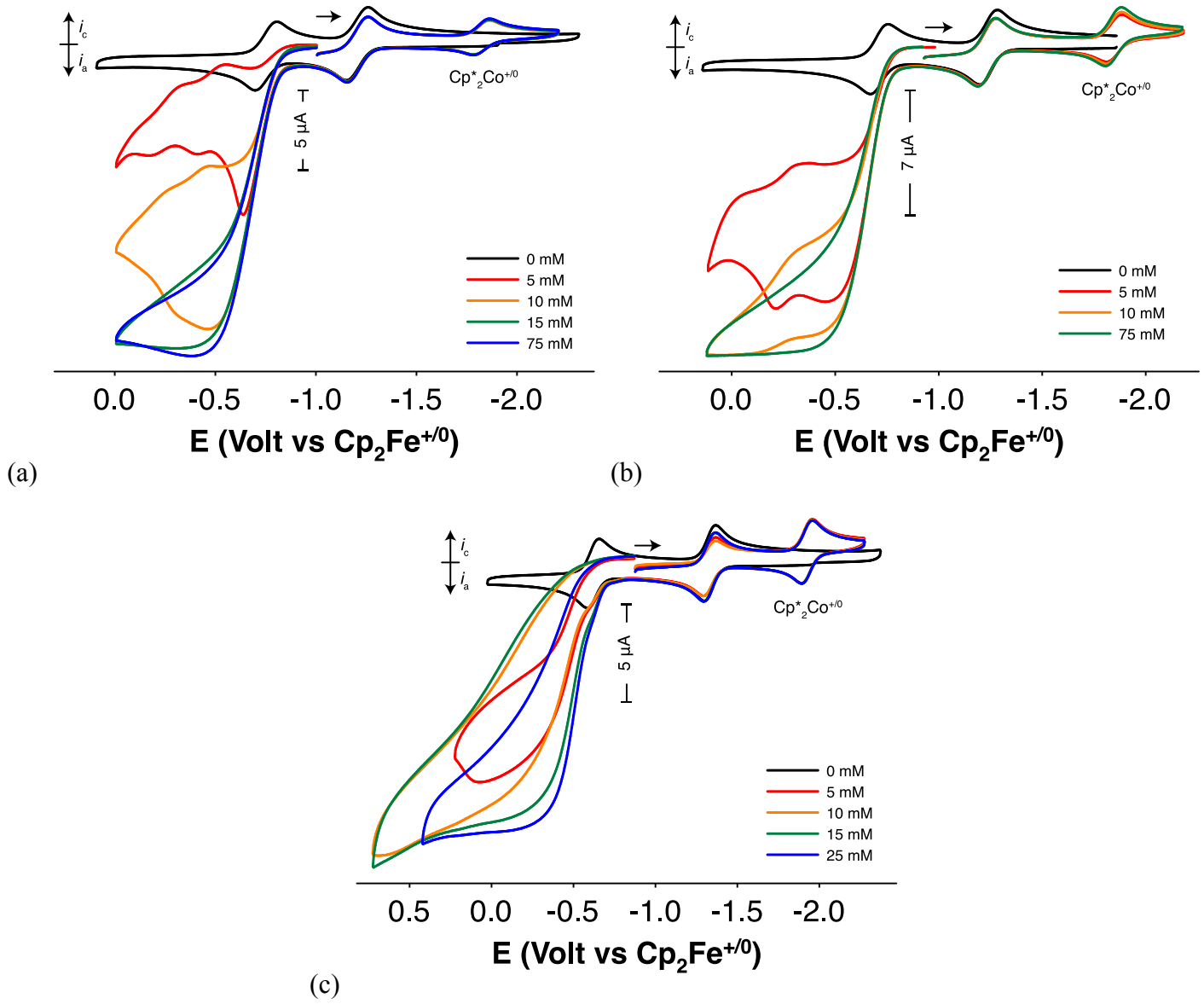

Figure S10. Cyclic volatammograms of a THF solution of $Ni(P^{Cy}_2N^{Bn}_2)_2$ upon addition of ^{n}BuNH$_2$ using (a) [^{n}Bu$_4$N][BF$_4$], (b) [^{n}Bu$_4$N][PF$_6$], and (c) [^{n}Bu$_4$N][B(C$_6$F$_5$)$_4$] as the supporting electrolyte. Conditions: 0.8 mM [Ni], 0.2 M electrolyte, 250 mV/s. Potentials are referenced to $Cp_2Fe^{+/0}$.

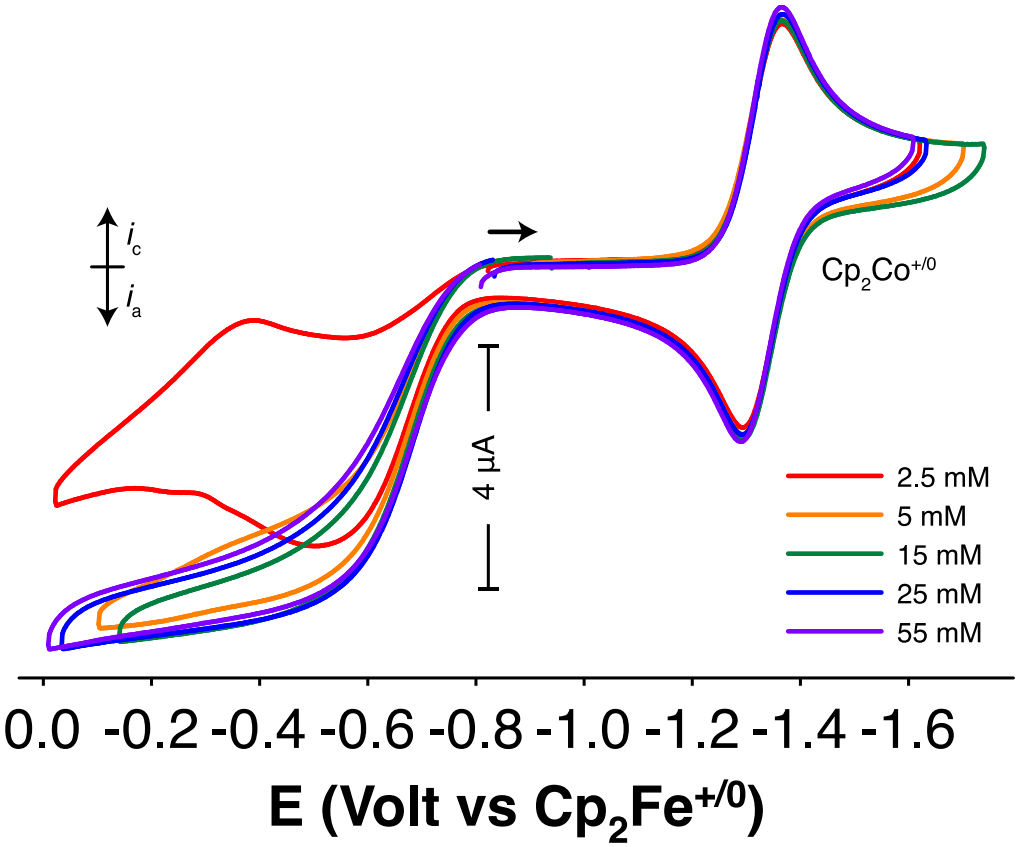

Figure S11. Cyclic volatommograms of a PhCN solution of $Ni(P^{Cy}{}_2N^{Bn}{}_2)_2$ upon addition of $^{n}BuNH_2$ using $[^{n}Bu_4N][PF_6]$ as the supporting electrolyte. Conditions: 0.8 mM [Ni], 0.2 M electrolyte, 250 mV/s. Potentials are referenced to $Cp_2Fe^{+/0}$.

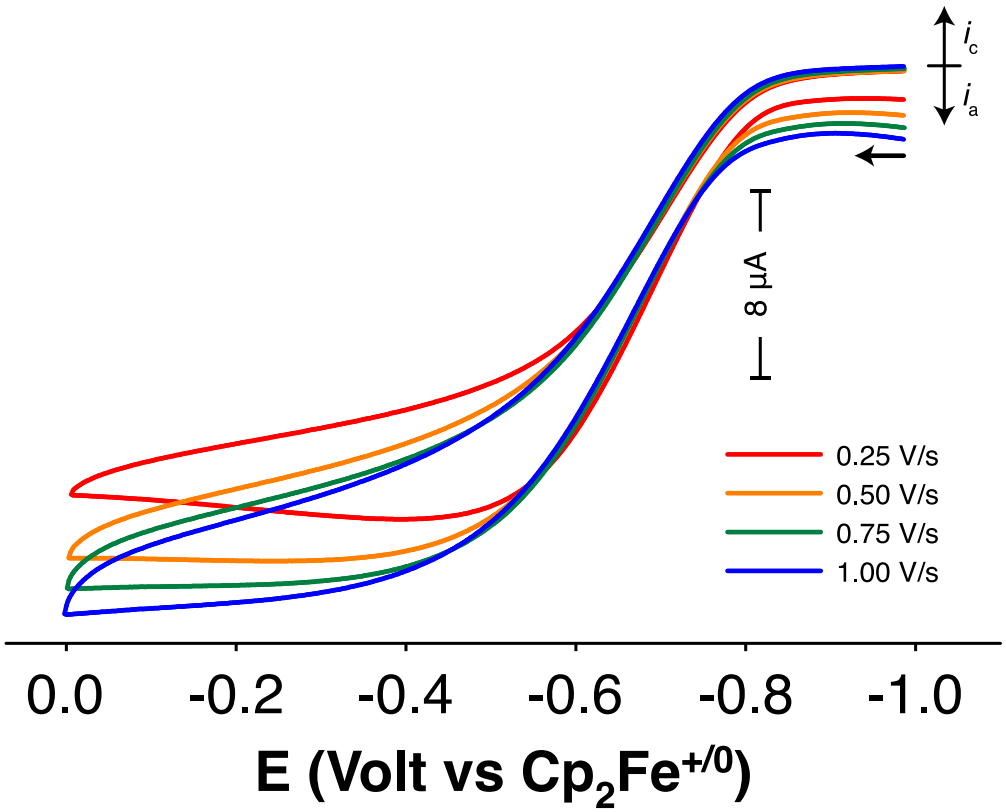

Figure S12. Cyclic volatommograms of a THF solution of $Ni(P^{Cy}{}_2N^{Bn}{}_2)_2$ as a function of scan rate. Conditions: 0.8 mM [Ni], 0.2 M [^{n}Bu$_4$N][BF$_4$], 90 mM ^{n}BuNH$_2$. Potentials are referenced to $Cp_2Fe^{+/0}$.

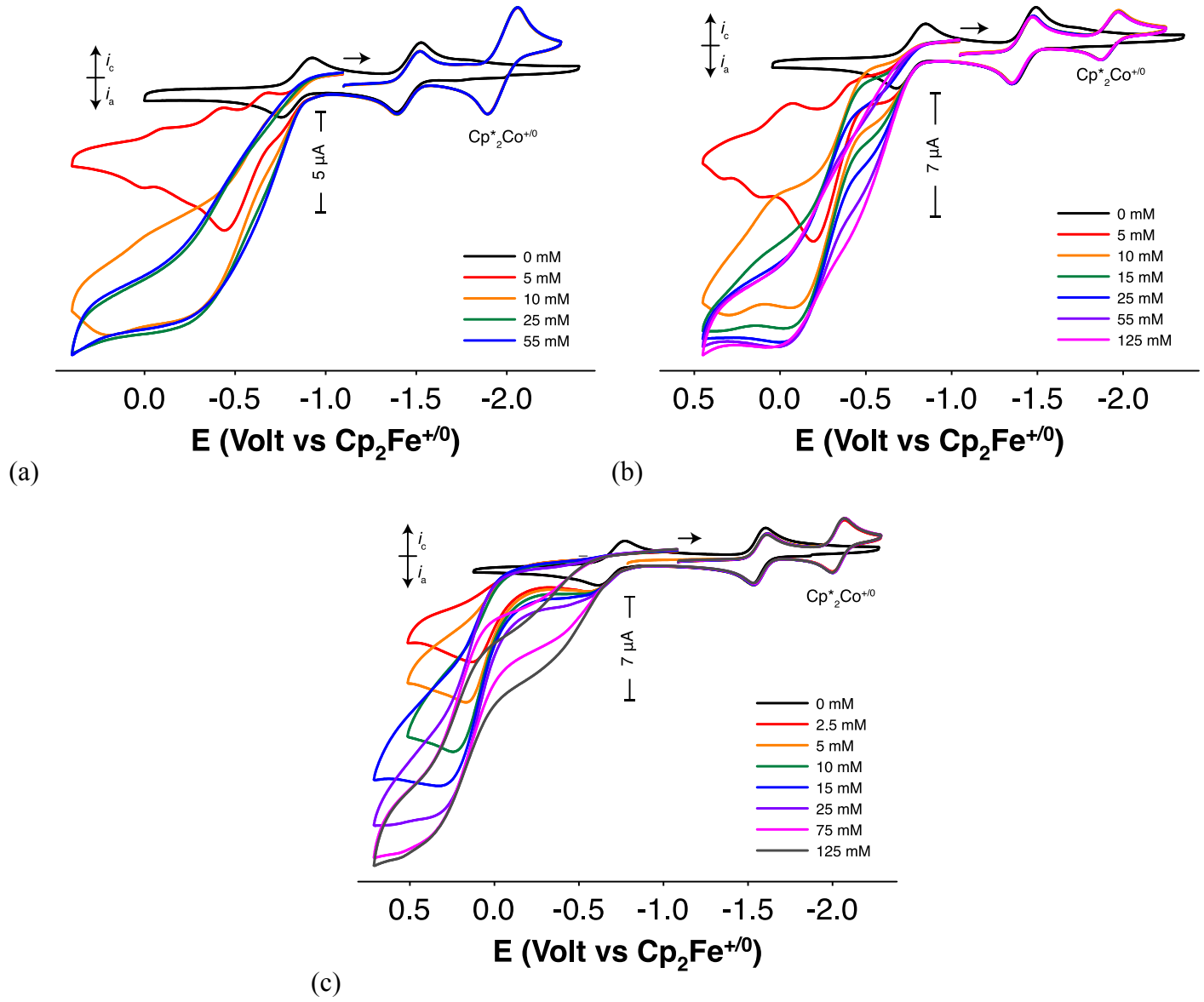

Figure S13. Cyclic volatammograms of a fluorobenzene solution of $Ni(P^{Cy}_2N^{tBu}_2)_2$ upon addition of ^{n}BuNH$_2$ using (a) [^{n}Bu$_4$N][BF$_4$], (b) [^{n}Bu$_4$N][PF$_6$], and (c) [^{n}Bu$_4$N][B(C$_6$F$_5$)$_4$] as the supporting electrolyte. Conditions: 0.8 mM [Ni], 0.2 M electrolyte, 250 mV/s. Potentials are referenced to $Cp_2Fe^{+/0}$.

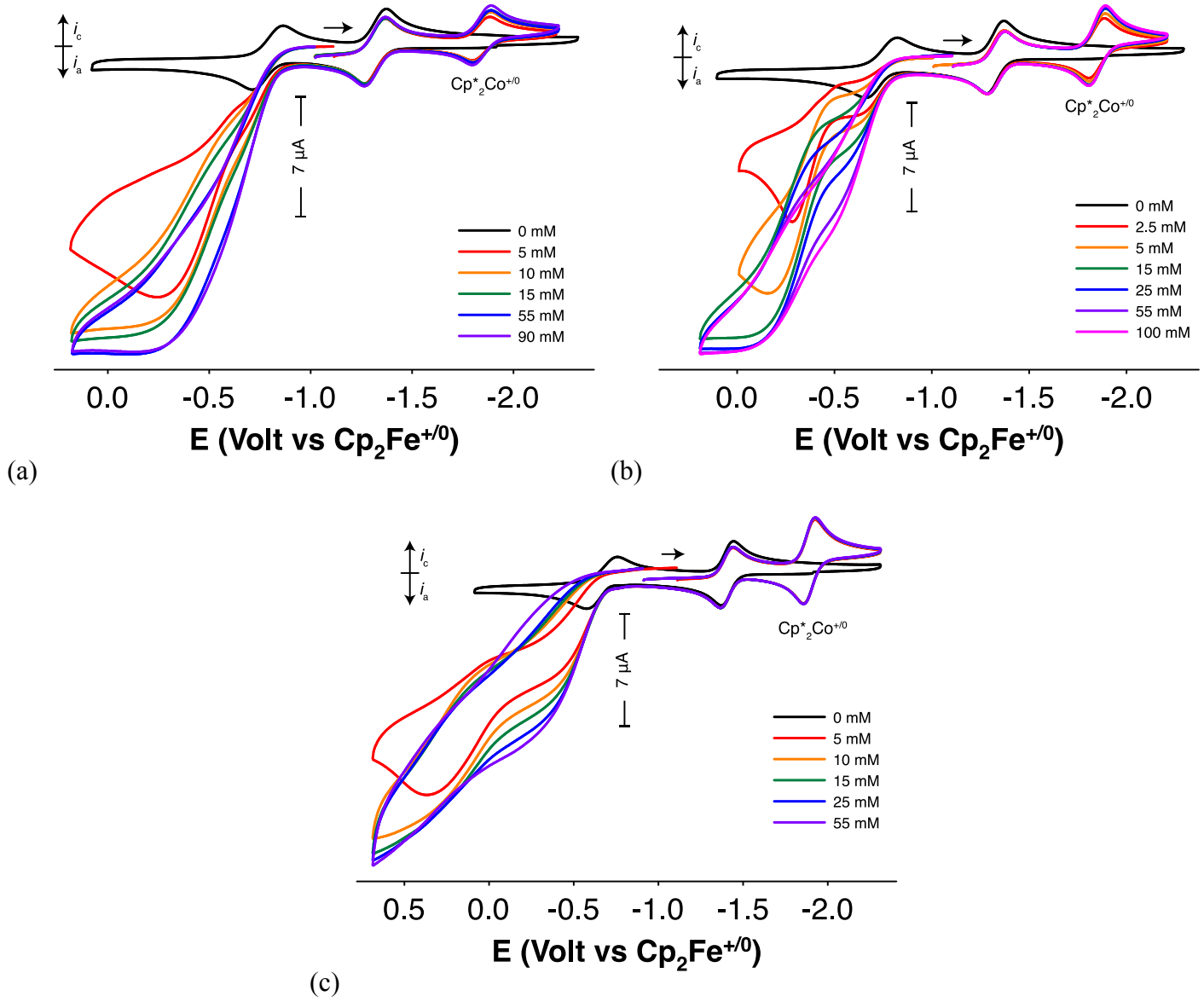

Figure S14. Cyclic volatammograms of a THF solution of $Ni(P^{Cy}_2N^{tBu}_2)_2$ upon addition of ^{n}BuNH$_2$ using (a) [^{n}Bu$_4$N][BF$_4$], (b) [^{n}Bu$_4$N][PF$_6$], and (c) [^{n}Bu$_4$N][B(C$_6$F$_5$)$_4$] as the supporting electrolyte. Conditions: 0.8 mM [Ni], 0.2 M electrolyte, 250 mV/s. Potentials are referenced to $Cp_2Fe^{+/0}$.

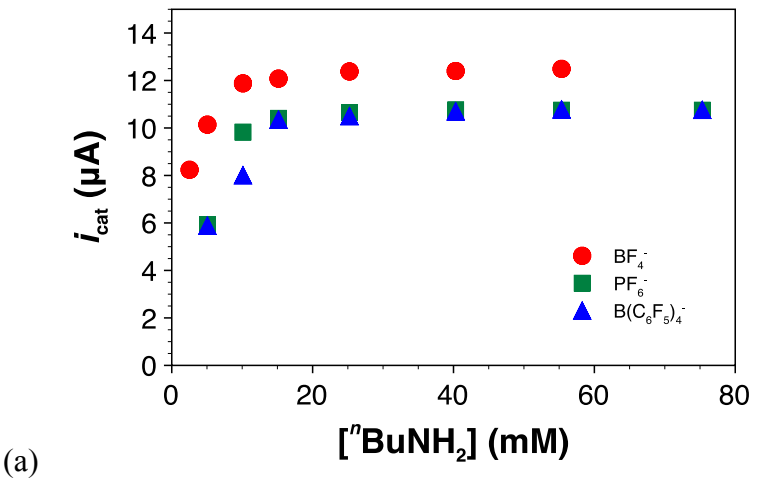

(a)

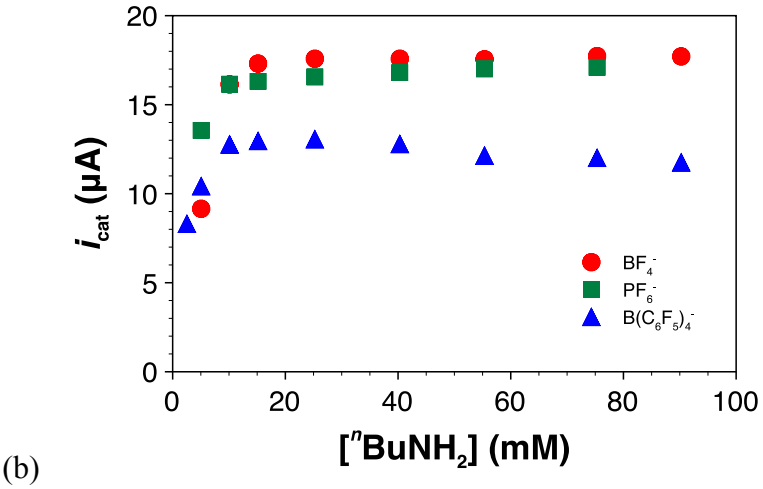

(b)

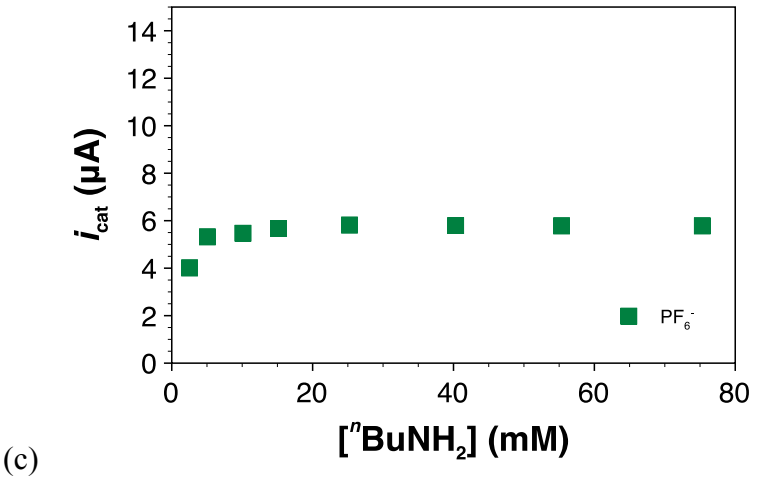

(c)

Figure S15. Plot of the catalytic current (i_{cat}) of Ni($P^{Cy}_2N^{Bn}_2$)$_2$ versus the concentration of ^{n}BuNH$_2$ in (a) fluorobenzene, (b) THF, and (c) benzonitrile solution using [^{n}Bu$_4$N][BF$_4$] (red circle), [^{n}Bu$_4$N][PF$_6$] (green square), and [^{n}Bu$_4$N][B(C$_6$F$_5$)$_4$] (blue triangle) as the supporting electrolyte. Conditions: 0.8 mM [Ni], 0.2 M electrolyte, 250 mV/s.

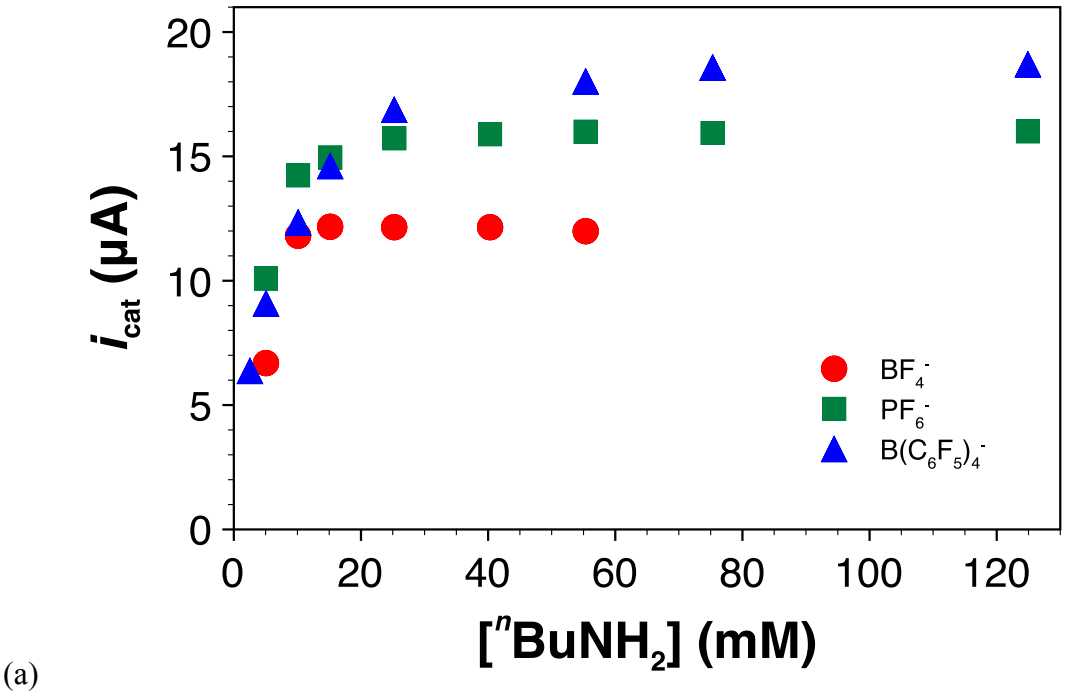

(a)

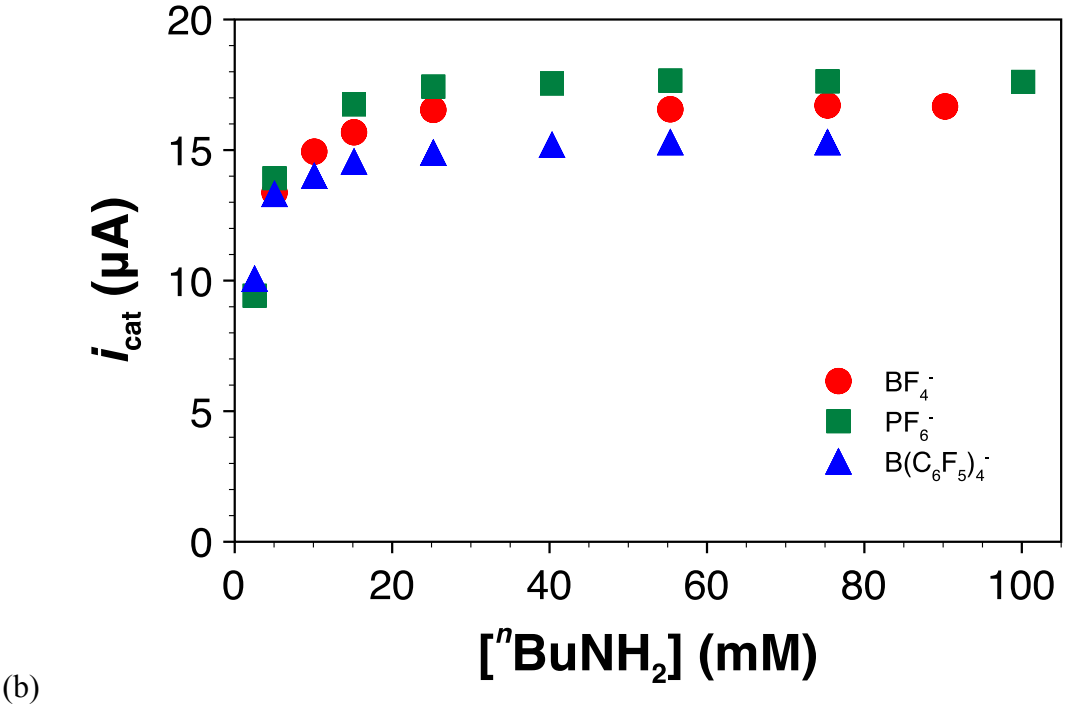

(b)

Figure S16. Plot of the catalytic current (i_{cat}) of Ni($P^{Cy}_2N^{tBu}_2$)$_2$ versus the concentration of ^{n}BuNH$_2$ in (a) fluorobenzene and (b) THF solution using [^{n}Bu$_4$N][BF$_4$] (red circle), [^{n}Bu$_4$N][PF$_6$] (green square), and [^{n}Bu$_4$N][B(C$_6$F$_5$)$_4$] (blue triangle) as the supporting electrolyte. Conditions: 0.8 mM [Ni], 0.2 M electrolyte, 250 mV/s.

References:

1. M. O'Hagan, W. J. Shaw, S. Raugei, S. Chen, J. Y. Yang, U. J. Kilgore, D. L. DuBois, and R. M. Bullock, *J. Am. Chem. Soc.*, 2011, **133**, 14301–14312.
2. J. Y. Yang, S. Chen, W. G. Dougherty, W. S. Kassel, R. M. Bullock, D. L. DuBois, S. Raugei, R. Rousseau, M. Dupuis, and M. R. DuBois, *Chem. Commun.*, 2010, **46**, 8618.